Dissociative scattering of fast HeH$^+$ ions at glancing-angle incidence on a crystal surface

Y. Susuki, T. Ito, K. Kimura, and M. Mannami
Department of Engineering Science, Kyoto University, Kyoto 606-01, Japan
(Received 1 August 1994)

Kinetic energies and charge-state fractions of specularly reflected fragments have been studied at glancing-angle incidence of (0.8–2.5)-MeV HeH$^+$ ions on a clean (001) surface of SnTe. It is shown that the kinetic energies of fragments agree well with those calculated from Coulomb repulsion of He$^+$ and H$^+$ fragments, while most of the outgoing fragments are bare nuclei. The final kinetic energies and charge-state fractions of fragments are explained by a computer simulation: HeH$^+$ dissociates into fragments where at least one electron is retained in the He-H system and there follows electron loss from the fragments after most of the initial potential energy has been transferred to the kinetic energies of fragments. The cross section for dissociation of HeH$^+$ ions in collisions with electrons at the surface is estimated to be of the order of 10^{-16} cm^2.

PACS number(s): 79.20.Rf, 34.50.Gb, 34.70.+e, 34.80.Gs

I. INTRODUCTION

The process of dissociation of fast molecular ions interacting with solids is of great scientific and technical interest. Fragmentation of MeV molecular ions has been intensively investigated in collisions with thin foils or gas atoms [1,2]. In the foil-induced fragmentation, rapid electron loss of the projectile occurs at the incident surface of the foil and there follows a "Coulomb explosion" of the projectile on a much longer time scale. The fragments are distributed on an ellipse on the joint distribution in energy and angle of emergence. Polarization wake potentials induced by the fragments also influence the motion of the fragments. For example, at the incidence of MeV HeH$^+$ ions, the H$^+$ fragments trailing He partners are strongly enhanced by the attractive force of wakes of He ions [1,2].

We have previously reported results for the angular and energy distributions of the fragments for glancing-angle incidence of MeV H$_2^+$ and HeH$^+$ ions on a clean (001) surface of SnTe [3,4]. The geometry of the scattering is not symmetric around the beam axis, which is different from that with foil-induced fragmentation. The internuclear vectors connecting the exploding fragments are influenced by the geometry. They tend to be parallel to the surface during the dissociation under the influence of the surface continuum potential. Similar experimental studies have been reported by Winter, Poizat, and Remillieux, where the energy of the fragments is measured with a high-resolution electrostatic spectrometer [5].

Recently we improved the energy resolution of our ion detecting system and reported the distributions of fragments in energy and angle when MeV HeH$^+$ ions dissociate at glancing-angle incidence on a clean surface of SnTe [6]. A distribution corresponding to the "ring pattern" of the fragments observed at the foil-induced fragmentation is obtained when the angular dependence of the energy spectra is measured in the direction parallel to the surface. That is, the fragments are approximately distributed on an ellipse in the E-ϕ plane, where E is the energy of the fragments and ϕ is the scattering angle measured parallel to the surface. Further, the trailing H$^+$ fragments are strongly enhanced and the enhancement represents the influence of surface wakes induced by the He fragments of the partners. On the other hand, only the leading and trailing fragments can be observed in the E-θ plane at $\phi=0$, where θ is the angle of scattering measured in the scattering plane. The energy separation of the leading and trailing H$^+$ fragments in the E-θ plane is equal to the diameter along the E axis of the ellipse in the E-ϕ plane. The experimental E-ϕ and E-θ distributions are well reproduced by a computer simulation of the dissociative scattering of HeH$^+$ ions, where surface-wake potentials and the charge exchange of fragments are considered [7]. The experimental and simulated distributions show that the internuclear vector of the fragments tends to be parallel to the surface during the dissociation due to the influence of the surface planar potential. The fragments repel each other in a plane parallel to the surface.

It has been indicated in Ref. [7] that the diameter of the ellipse in the E-ϕ plane is useful to estimate the cross section for dissociation of HeH$^+$ ions in collisions with electrons at the surface. In the present paper, we report the dependence of the diameters of the ellipse along the E axis on the energy of incidence ranging from 0.8 to 2.5 MeV, for glancing-angle incidence of HeH$^+$ ions on a clean (001) surface of SnTe. Computer simulation of the angular and energy distributions of scattered fragments is also carried out in order to explain the measured diameter and to obtain the cross section for dissociation of HeH$^+$ ions in collisions with electrons at the surface.

II. EXPERIMENTAL PROCEDURE

The main part of the experimental setup was described elsewhere [6,8], so only relevant points of the experimental procedure are mentioned here.

A magnetically analyzed beam of MeV HeH$^+$ ions from the 4-MV Van de Graaff accelerator of Kyoto University was collimated to have a maximal angular diver-

gence of ± 0.1 mrad and introduced to a UHV scattering chamber through a differentially pumped section. The target was a single crystal of SnTe (100), which was prepared by *in situ* evaporation of pure SnTe (purity 99.999%) on a KCl (100) surface under UHV conditions. The angle of incidence of the ions relative to the surface plane, θ_i, was less than 11 mrad. The azimuthal angle of the incident beam was adjusted so that surface channeling of the projectile did not occur.

The energy spectra and the charge-state distributions of the scattered fragments were measured at the angle of specular reflection with a magnetic spectrometer (the relative energy resolution of the spectrometer was 0.5%) or a solid state detector (PD25-10-500 AM, Canberra Industries, Inc.). The acceptance half angle of the magnetic spectrometer was ± 0.1 mrad and that of the solid-state detector was ± 0.3 mrad.

III. EXPERIMENTAL RESULTS

A. Charge-state fractions of fragments

The incidence-energy dependence of the charge-state fractions for the H and He fragments in the scattered beam is shown in Fig. 1, where the angle of incidence of the HeH⁺ ions is 4 mrad. The fractions of the HeH⁺ and H⁻ ions in the scattered ions were less than 10^{-4}.

We measured the dependence of the charge-state fractions for the fragments on the angle of incidence. The charge-state fractions for He⁺ and He²⁺ in the scattered He fragments are shown by circles in Fig. 2 for 0.8- and 1.6-MeV HeH⁺ ions incident. The charge-state fractions are almost constant. The charge-state fractions for He⁰ and H⁰ in the scattered fragments were of the order of 10^{-2}.

B. Energy spectra of H⁺ fragments

An example of the energy spectra for H⁺ fragments arising from dissociation of 0.8-MeV HeH⁺ ions is shown in Fig. 3, where the angle of incidence was 6.4 mrad. Two peaks are seen in the spectrum. The higher-energy peak corresponds to H⁺ fragments leading the He fragments of their partners and the lower-energy peak corresponds to H⁺ fragments trailing their partners [6]. The yield of the ions in the lower-energy peak is larger than that of the higher-energy peak. The enhancement of the lower-energy peak represents the influence of the surface wakes induced by He fragments of the pairs [6]. The energy separation between the leading and trailing H⁺, ΔE, is calculated from the difference in peak energies.

We have measured the dependence of the energy separation on the angle of incidence, which is shown in Fig. 4 by circles for 0.8- and 1.6-MeV HeH⁺ ions. The mea-

FIG. 1. Dependence of the charge-state fractions for fragments in the beam scattered at the angle of specular reflection on the energy of incident HeH⁺ ions, where the angle of incidence is 4 mrad.
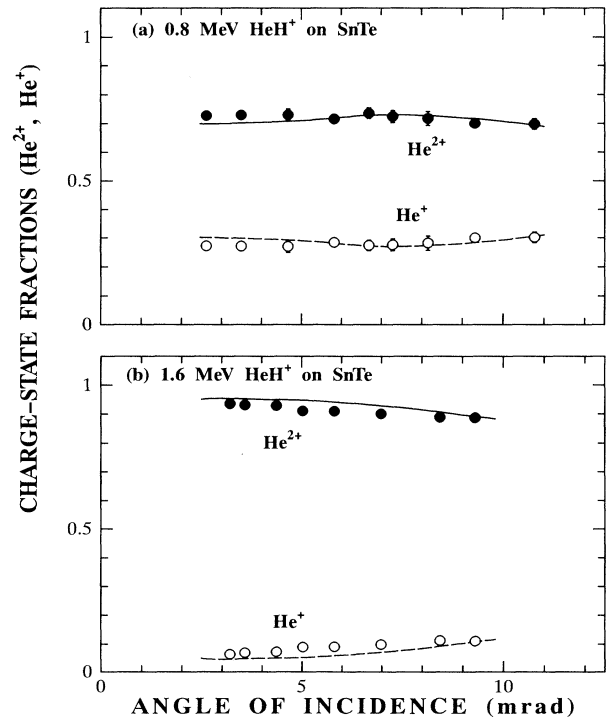
FIG. 2. Dependence of the charge-state fractions of He⁺ and He²⁺ in the He ions scattered at the angle of specular reflection on the angle of incidence. (a) The energy of incident HeH⁺ ions is 0.8 MeV. (b) The energy of incident HeH⁺ ions is 1.6 MeV. The circles show the experimental results and the lines show the simulated results.
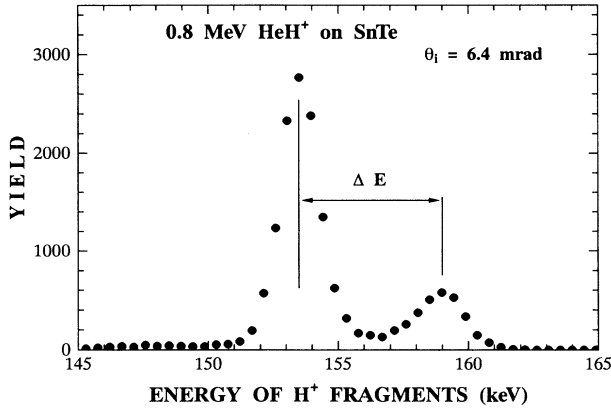
FIG. 3. An example of the energy spectra of H^+ scattered at the angle of specular reflection, where the energy of incident HeH^+ is 0.8 MeV and the angle of incidence is 6.4 mrad.

sured separation does not depend on the angle of incidence at angles less than 7 mrad. The incidence-energy dependence of the energy separation has been measured for an incidence angle of 3.5 ± 0.6 mrad. The experimental error in the angle of incidence does not influence the energy separation. We show the measured separation by
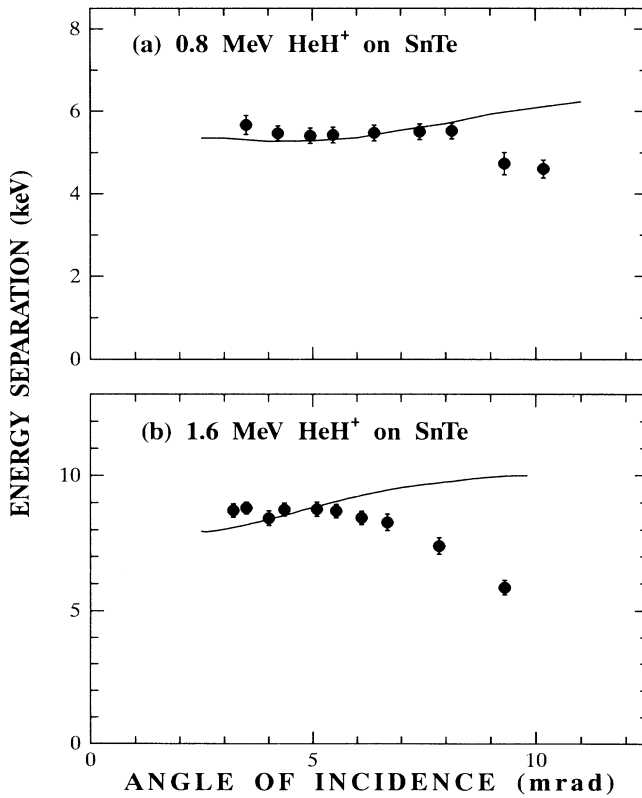
FIG. 4. Dependence of the energy separation between the leading and the trailing H^+ on the angle of incidence (a) for 0.8-MeV HeH^+ ion incidence and (b) for 1.6-MeV HeH^+ ion incidence. The circles show the experimental results and the lines show the simulated ones.
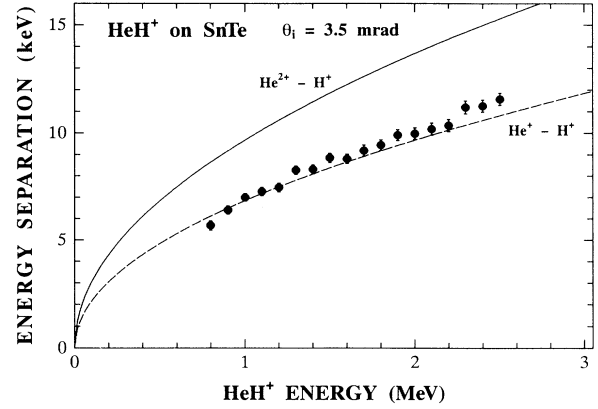
FIG. 5. Dependence of the energy separation between the leading and the trailing H^+ on the energy of incident HeH^+ ions, where the angle of incidence is 3.5 ± 0.6 mrad. The two parabolic lines are calculated energy separations for the He^{2+}-H^+ and He^+-H^+ states in free space.

closed circles in Fig. 5. The energy separation increases with increasing energy of incidence.

IV. COMPUTER SIMULATION

A. Coulomb explosion in free space

In free space, the mutual Coulomb energy of a pair of fragments He^{p+} and H^+ is expressed as

$$U = \frac{pe^2}{R_0} , \qquad (1)$$

where R_0 is the internuclear distance of HeH^+ in the incident beam. Using the most probable value $R_0 = 0.79$ Å [1,2], we obtain the energy $U = 36.5$ and 18.2 eV for He^{2+}-H^+ and He^+-H^+ pairs, respectively. This potential energy is converted into kinetic energy as the dissociation develops. The final velocity in the c.m. frame $|v|$ acquired by the H^+ ion is

$$|v| = \frac{\sqrt{2\mu U}}{M} , \qquad (2)$$

where μ is the reduced mass of the two fragments and M is the mass of H^+. The energy separation between the leading and trailing H^+ in the laboratory frame is then

$$\Delta E \simeq 2M|V||v| = 2|V|\sqrt{2\mu U} = \tfrac{8}{5}\sqrt{E_I U} , \qquad (3)$$

where V and E_I are the velocity and the energy of the incident HeH^+, respectively.

The measured energy separations shown in Fig. 5 are compared with the calculated ones using Eq. (3), where the calculated energy separations for He^2-H^+ and He^+-H^+ pairs are shown by lines. The measured energy separations agree well with the calculations for He^+-H^+ pairs. However, most of the measured fragments are He^{2+} and H^+ as shown in Figs. 1 and 2. In order to explain the observed energy separation and the charge-state fractions of fragments, a computer simulation was carried out.

B. Procedure for the computer simulation

We calculated more than 10^4 trajectories for randomly oriented MeV HeH$^+$ ions and their fragments for a range of conditions of the energy and angle of incidence. We obtained the simulated outgoing velocity distribution and the charge-state distributions of the fragments. In the computer simulation, we made several approximations for the dissociative scattering process of HeH$^+$ ions. The procedures for the computer simulation were as follows.

The (001) surface of SnTe was assumed to be atomically flat. The trajectories of randomly oriented HeH$^+$ projectiles were calculated using a surface-continuum potential derived from the Molière approximation for the screening function of Thomas-Fermi type. The internuclear distance of incident HeH$^+$ was 0.79 Å and fixed before the start of dissociation.

The trajectory of each dissociated fragment was calculated using the surface-continuum potential, repulsive potential for the fragment of a pair, and the surface-wake potential induced by the fragment from a pair. For the repulsive potential between the fragments, we used the diagram of interaction potentials of the He-H system [9]. For the surface-wake potential, a formalism derived for the ion moving parallel to a surface of semi-infinite medium was used [6,10,11].

The HeH$^+$ projectile is excited on its trajectory to one of its excited states by collisions with electrons at the surface and starts to dissociate into a pair of fragments. The electron distribution outside the surface was calculated by averaging those of isolated Sn and Te atoms in a plane parallel to the surface [12]. The cross section σ_E for the excitation of HeH$^+$ ions in collisions with electrons was taken as a parameter to fit the simulated velocity distribution of the H$^+$ fragments to the observed one. Since we could not deal with all of the excited states for the initial excitation, we chose the $a\,^3\Sigma^+$, $A\,^1\Sigma^+$, $1s\sigma$, and fully ionized (He^{2+}-H$^+$) states as representative states, where H^0 and He$^+$ arise from the $a\,^3\Sigma^+$ and $A\,^1\Sigma^+$ states and H$^+$ and He$^+$ arise from the $1s\sigma$ state.

The fragments undergo charge-exchange collisions with the surface atoms. The position-dependent probabilities of electron loss and electron capture of fragment as calculated by the Bohr and Bohr-Lindhard models for atomic ions were used [13,14]. Since the fraction of He^0 is negligibly small compared with those of He$^+$ and He^{2+}, we neglected electron capture by He$^+$.

Energy losses of the fragments were calculated with the use of an empirical formula for the position-dependent stopping power for atomic ions [15]. The formula is regarded as the sum of stopping powers for individual and collective excitations of target electrons. Therefore the stopping of a fragment by the wake induced by itself was not calculated. Small-angle multiple-scattering events due to electronic and nuclear collisions were neglected.

The final result for the velocity distribution of the H$^+$ fragments was convoluted with a three-dimensional Gaussian distribution which had appropriate widths in energy E and angles θ and ϕ. From the convoluted velocity distribution, the energy spectrum of H$^+$ fragments at the angle of specular reflection was obtained.

C. The best-fit excitation cross sections

Figure 6 shows an example of a simulated energy spectrum of H$^+$ fragments emerging at the angle of specular reflection, where 0.8-MeV HeH$^+$ ions are incident with $\theta_i = 6.25$ mrad. The $a\,^3\Sigma^+$ state is chosen for the initial excitation and the cross section for excitation is assumed to be 2×10^{-16} cm^2. The simulated energy spectrum shows the leading and trailing peaks similar to the experimental spectrum shown in Fig. 3. However, the energy separation between the leading and trailing protons depends on the state chosen for the initial excitation and the excitation cross section. Therefore the excitation cross section is obtained from a comparison of the experimental and simulated energy separation.

Examples of the procedure to obtain the best-fit excitation cross sections are shown in Fig. 7. The hatched area in Fig. 7 shows the experimental energy separation and its error. The states chosen for the initial excitation are indicated. For the $a\,^3\Sigma^+$ and $A\,^1\Sigma^+$ states, the simulated energy separation decreases with increasing cross section and crosses the hatched area. The best-fit cross section for excitation is obtained by searching the cross section where the simulated energy separations are within the hatched area. For the He^{2+}-H$^+$ state, the simulated energy separation is larger than the experimental one. This shows that most of the projectiles are not excited to the He^{2+}-H$^+$ state at the initial excitation. For the $1s\sigma$ state, which is formed by electron loss from HeH$^+$, the best-fit cross section is obtained in a similar way as that for the $a\,^3\Sigma^+$ and $A\,^1\Sigma^+$ states at energies of incidence larger than 1.2 MeV. However, the peak for the leading fragments contains two components at energies of incidence less than 1.2 MeV. The high-energy component in the peak for the leading H$^+$ fragments is not observed
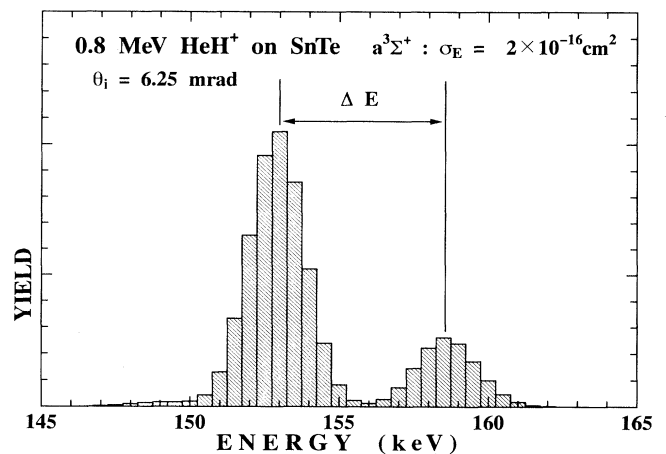
FIG. 6. An example of the simulated energy spectra of H$^+$ emerging at the angle of specular reflection, where the energy of incident HeH$^+$ is 0.8 MeV and the angle of incidence is 6.25 mrad. The $a\,^3\Sigma^+$ state is chosen for the initial excitation and the cross section for the excitation is assumed to be 2×10^{-16} cm^2 in the simulation. The Gaussian distribution used for the convolution has full widths at half maximum of 2 keV, 4 mrad, and 3 mrad in energy, in the ϕ and θ directions, respectively.
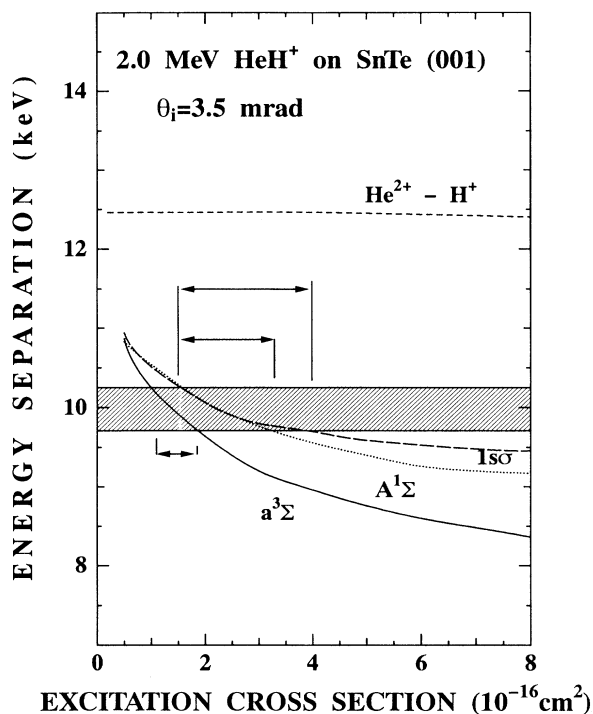
FIG. 7. Dependence of the simulated energy separations on the assumed cross section for excitation to the $a\,^3\Sigma^+$, $A\,^1\Sigma^+$, $1s\sigma$, and He^{2+}-H^+ states at 2.0-MeV HeH^+ incidence with $\theta_i = 3.5$ mrad. The hatched area shows the experimental energy separation and its error.
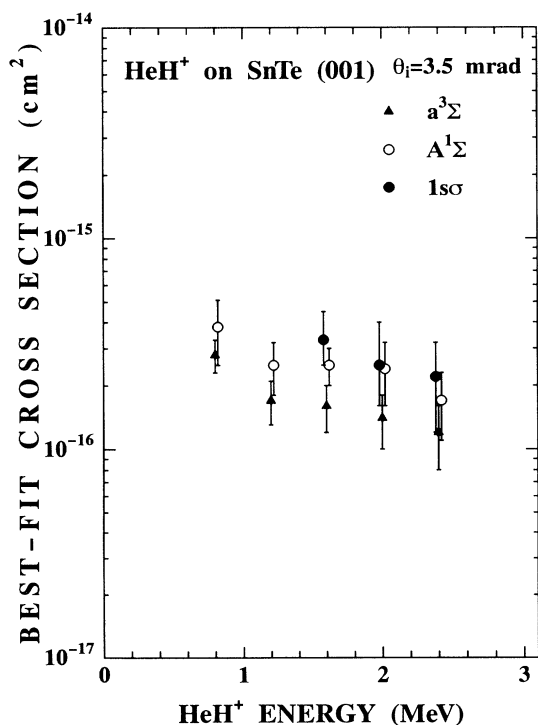
FIG. 8. Best-fit cross sections for excitation of HeH^+ ions to the $a\,^3\Sigma^+$, $A\,^1\Sigma^+$, and $1s\sigma$ states in collisions with electrons at the surface.

in the experimental spectrum. The high-energy component arises from fragments repelled away from the surface by repulsion of He fragments, whose molecular axes are oriented to the surface with the He^+ closer to the surface [6]. This shows that most of the projectiles are not excited to the $1s\sigma$ state at energies of incidence less than 1.2 MeV and that the projectiles are excited without loss of electrons (e.g., the $a\,^3\Sigma^+$ or the $A\,^1\Sigma$ state).

The best-fit cross sections for excitation to the three states for several energies of incident HeH^+ ions are shown in Fig. 8. They are not so different and are of the order of 10^{-16} cm^2.

V. DISCUSSION

A. Process of dissociative scattering of HeH^+ ions

Although most of outgoing fragments are He^{2+} and H^+, the experimental energy separation between the leading and trailing H^+ fragments agrees well with the energy separation calculated assuming dissociation of He^+-H^+ pair in free space as shown in Fig. 5. The apparent contradiction was explained by the computer simulation as follows. The HeH^+ projectiles dissociate on their incoming trajectory in collisions with the electrons at the surface via excited states of the He-H system where at least one electron is retained. The fragments repel each other, while the internuclear vectors become parallel to the surface under the influence of the surface potential. After the major part of the initial potential energy of the fragment pair is converted to kinetic energy, the charge exchange occurs and the binding electrons are lost from the fragments. Thus most of fragments are reflected from the surface as bare nuclei and the energy separation agrees with that calculated assuming dissociation of the He^+-H^+ pair in a free space.

B. Cross section for dissociation of HeH^+ ions in collisions with electrons

It has been shown from the simulation that the excitation cross sections of HeH^+ to the $a\,^3\Sigma^+$, $A\,^1\Sigma^+$, and $1s\sigma$ states are of the order of 10^{-16} cm^2. We forbid the excitation to states other than the selected one in the simulation. However, there are many other excited states that lead to He^+ and H^0 pairs or He^+ and H^+ pairs. The interaction potential curves for these states are almost the same as those of the $a\,^3\Sigma^+$, $A\,^1\Sigma^+$, and $1s\sigma$ states [9,16–20]. Therefore, if one of these states is chosen instead of the $a\,^3\Sigma^+$, $A\,^1\Sigma^+$, and $1s\sigma$ states, the simulation will give the same cross section for the excitation. Thus we could not find the excitation cross section to each state; however, the cross section for dissociation of HeH^+ by electron collision is of the order of 10^{-16} cm^2. We estimated the cross section for dissociation by averaging the best-fit cross sections shown in Fig. 8 and the cross sections are shown in Fig. 9 by circles.

In order to compare the cross section for dissociation of HeH^+ with those for other reactions induced by impact of electrons, the upper scale of Fig. 9 is transformed to the energy of electrons that have the same velocity
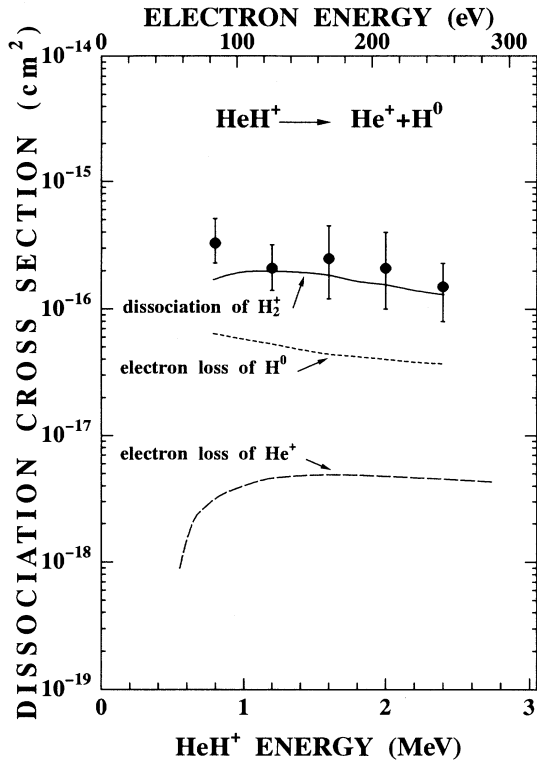
FIG. 9. Cross section for dissociation of HeH$^+$ ions in collisions with electrons at the surface. The upper scale shows the energy of electrons of the same velocity with HeH$^+$ ions. The solid line shows the dissociation cross section of H$_2^+$ ions [21], the dotted line shows the electron-loss cross section of H^0 atoms [22], and the dashed line shows the electron-loss cross section of He$^+$ ions [23].

with HeH$^+$ ions. The solid line in Fig. 10 shows the dissociation cross section for H$_2^+$ ions [21], the dotted line shows the electron-loss cross section for H^0 atoms [22], and the dashed line shows the electron-loss cross section for He$^+$ ions [23]. The cross sections range from about 10^{-18} to about 10^{-16} cm^2. Our estimated cross sections are close to the dissociation cross section for H$_2^+$ ions in the present range of electron-impact energy. Yousif and Mitchell have measured the dissociation cross section for HeH$^+$ ions with the impact of electrons whose energies are less than 40 eV [24]: The measured cross section is of the order of 10^{-16} cm^2 for 20- and 26-eV incident electrons, where the electron energies correspond to the excitation of HeH$^+$, $X\,^1\Sigma^+ \Longrightarrow a\,^3\Sigma^+$, and $A\,^1\Sigma^+$, respectively. However, a comparison of their data with ours cannot be made directly because their impact energies are lower than ours.

C. Dependence of energy separation and charge-state fractions on the angle of incidence

We have simulated the dependence of the energy separation and the charge-state fractions on the angle of incidence. We have used here the estimated dissociation cross section. Since the energy separation is not very
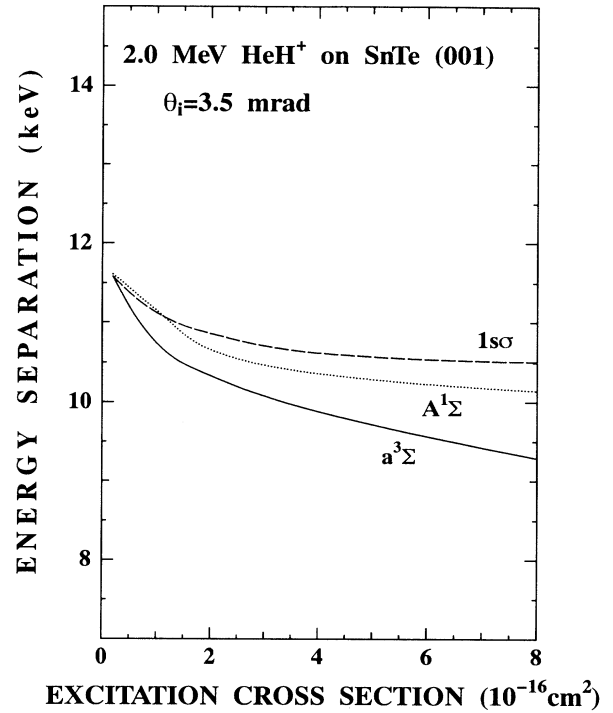
FIG. 10. Dependence of the simulated energy separations on the assumed cross section for excitation to the $a\,^3\Sigma^+$, $A\,^1\Sigma^+$, and $1s\sigma$ states. The surface wake potential was not used in this simulation.

state dependent, we assumed the $a\,^3\Sigma^+$ state for the initial excitation.

The simulated dependence of the energy separation on the angle of incidence is shown in Fig. 4 by solid lines. The simulated results deviate from the experimental ones for angles of incidence larger than several mrad, where the experimental ones decrease. The deviation is probably related to the multiple-scattering process, which is not treated in our simulation.

We compare the simulated charge-state fractions for the outgoing fragments with those obtained by experiments. The simulated charge-state fractions for the He fragments are shown in Fig. 2. The agreement between the experimental and simulated fractions is fairly good. The charge-state fraction is insensitive to the cross section because charge-state equilibrium is almost attained. In the simulation, most of the H fragments reflected at the angle of specular reflection were H$^+$.

D. Interpretation of energy separations obtained by the simulation

The energy separation obtained in the above simulation is closely related to the charge states of the fragments. The energy separation can be interpreted as follows.

We define a trajectory-dependent internuclear vector $R(x(R_0;z,p,q))$ from the nucleus of fragment He^{p+} to that of H^{q+} when the c.m. of the fragments is at (x,z) on a trajectory $x(R_0;z,p,q)$, where R_0 is the initial internu-

clear vector and the z axis and the x axis are parallel to the beam direction and the surface normal, respectively. The interaction potential between the fragments depends on the charge states and is expressed by $U_{pq}(\mathbf{R}(x))$. Charge states of the fragments change along the trajectory and the probabilities of finding He^{p+} and H^{q+} fragments at (x,z) on a trajectory $x(\mathbf{R}_0;z,p,q)$ are expressed by $F_p(z,\mathbf{R}_0)$ and $G_q(z,\mathbf{R}_0)$, respectively. These probabilities at $z=\infty$ for fragments averaged over randomly oriented R_0 are the simulated charge-state fractions.

For the incidence of HeH^+ ions having an initial internuclear vector $\mathbf{R}_0$, the mean kinetic energy in the c.m. frame $U_{\mathrm{c.m.}}$ of H^+ fragments at $z=\infty$ is expressed as

$$U_{\mathrm{c.m.}}(\mathbf{R}_0)=\int_{\mathrm{traj}}\sum_{p,q}\left[-\frac{\mu}{M}\frac{\partial U_{pq}(|\mathbf{R}(x)|)}{\partial|\mathbf{R}|}+W_{pq}(\mathbf{R}(x))\right]$$
$$\times F_p(z,\mathbf{R}_0)G_q(z,\mathbf{R}_0)$$
$$\times\frac{d|\mathbf{R}(x)|}{dx}\frac{dx}{dz}dz\ ,\qquad(4)$$

where μ is the reduced mass of the He-H system, M is the mass of H^+, and $W_{pq}(\mathbf{R}_0(x))$ is the force due to the surface wake acting on H^{q+} expressed in the c.m. system. Substituting this $U_{\mathrm{c.m.}}(\mathbf{R}_0)$ in U in Eq. (3), we obtain the energy separation $\Delta E(\mathbf{R}_0)$ for the HeH^+ ion with initial internuclear vector $\mathbf{R}_0$. The energy separation obtained in the simulation is the average of $\Delta E(\mathbf{R}_0)$ over randomly oriented $\mathbf{R}_0$. It is seen in Eq. (4) that not only the charge-exchange collision of fragments, but also the surface-wake potential induced by the He fragment affects the energy of the outgoing H^+ fragment of a pair.

The effect of the wake potential on the energy separation depends on the internuclear distance $R(x)$ of the fragments interacting with surface and the wavelength λ (roughly $23\sqrt{E}$ Å, where E is the energy of the HeH^+ in

MeV) of the wake potential. For internuclear distances smaller than $\lambda/4$, the wake forces are repulsive and increase the energy separation. If the internuclear distance is larger than $\lambda/4$, the wake forces decrease the energy separation. The energy separation simulated without wake potential is shown in Fig. 10 at 2.0-MeV HeH^+ incidence with $\theta_i=3.5$ mrad. A comparison between Figs. 7 and 10 shows that the wake potential reduces the energy separation. The effect of the wake potential depends on the excitation cross section. For the best-fit cross sections, it can be seen that the wake potential reduces the energy separation to about 0.9 times that calculated without wakes.

VI. CONCLUSION

We have studied the kinetic energies and charge-state fractions for fragments when HeH^+ ions are incident on (001) surface of SnTe with energies ranging from 0.8 to 2.5 MeV. The energy separation between the leading and trailing H^+ is related to the charge states of fragment and the surface-wake potential induced by the He fragment of a pair. The measured energy separations and charge-state fractions are reproduced by the computer simulation. An estimation of the cross section for dissociation of HeH^+ ions in collisions with electrons of surface is carried out. The estimated cross section is of the order of 10^{-16} cm^2 and comparable to the electron-impact dissociation cross section for H_2^+ ions.

[1] D. S. Gemmell, Chem. Phys. Rev. **80**, 301 (1980).

[2] D. S. Gemmell and Z. Vager, *Treatise on Heavy-Ion Science*, edited by D. A. Bromley (Plenum, New York, 1985), Vol. 6, p. 243.

[3] Y. Susuki, H. Mukai, K. Kimura, and M. Mannami, Nucl. Instrum. Methods B **48**, 347 (1990).

[4] Y. Susuki, H. Mukai, K. Kimura, and M. Mannami, J. Phys. Soc. Jpn. **59**, 1211 (1990).

[5] H. Winter, Radiat. Eff. **117**, 53 (1991); H. Winter, J. C. Poizat, and J. Remillieux, Nucl. Instrum. Methods B **67**, 345 (1992).

[6] Y. Susuki, T. Ito, K. Kimura, and M. Mannami, J. Phys. Soc. Jpn. **61**, 3535 (1992).

[7] Y. Susuki, T. Ito, K. Kimura, and M. Mannami, Nucl. Instrum. Methods B **90**, 310 (1994).

[8] M. Mannami, K. Kimura, K. Nakanishi, and A. Nishimura, Nucl. Instrum. Methods B **13**, 587 (1986).

[9] E. P. Kanter, P. J. Cooney, D. S. Gemmell, K. O. Groeneveld, W. J. Pietsch, A. J. Ratkowski, Z. Vager, and B. J. Zabransky, Phys. Rev. **20**, 834 (1979).

[10] N. Takimoto, Phys. Rev. **146**, 366 (1966).

[11] F. Flores and F. Garcia-Moliner, J. Phys. C **12**, 907 (1979).

[12] K. Kimura, Y. Fujii, M. Hasegawa, Y. Susuki, and M. Mannami, Phys. Rev. B **38**, 1052 (1988).

[13] N. Bohr and J. Lindhard, K. Dan. Vidensk. Selsk. Mat.-Fys. Medd. **28**, No. 7 (1954).

[14] Y. Fujii, K. Sueoka, K. Kimura, and M. Mannami, J. Phys. Soc. Jpn. **58**, 2758 (1989).

[15] K. Kimura, H. Hasegawa, and M. Mannami, Phys. Rev. B **36**, 7 (1987).

[16] H. H. Michels, J. Chem. Phys. **44**, 3834 (1966).

[17] T. A. Green, H. H. Michels, J. C. Browne, and M. M. Madsen, J. Chem. Phys. **61**, 5186 (1974).

[18] T. A. Green, H. H. Michels, J. C. Browne, and M. M. Madsen, J. Chem. Phys. **61**, 5198 (1974).

[19] T. A. Green, H. H. Michels, and J. C. Browne, J. Chem. Phys. **64**, 3951 (1976).

[20] T. A. Green, H. H. Michels, and J. C. Browne, J. Chem. Phys. **69**, 101 (1978).

[21] D. Mathur, J. B. Hasted, and S. U. Khan, J. Phys. B **12**, 2043 (1979).

[22] W. L. Fite and R. T. Brackmann, Phys. Rev. **112**, 1141 (1958).

[23] K. T. Dolder, M. F. A. Harrison, and P. C. Thonemann, Proc. R. Soc. London Ser. A **264**, 367 (1961).

[24] F. B. Yousif and J. B. A. Mitchell, Phys. Rev. A **40**, 4318 (1989).